Title

Myosin Id localizes in dendritic spines through the tail homology 1 domain

Authors

Ryusuke Koshida*, Saki Tome, Yosuke Takei*

Affiliations

Department of Anatomy and Neuroscience, Faculty of Medicine, University of Tsukuba, Tsukuba 305-8577, Japan

***Corresponding authors**

Email addresses: rkoshida@md.tsukuba.ac.jp (R. Koshida), ytakei@md.tsukuba.ac.jp (Y. Takei)

Abstract

Dendritic spines, the postsynaptic compartments at excitatory synapses, are capable of changing their shape and size to modulate synaptic transmission. The actin cytoskeleton and a variety of actin-binding proteins play a critical role in the dynamics of dendritic spines. Class I myosins are monomeric motor proteins that move along actin filaments using the energy of ATP hydrolysis. Of these class I myosins, myosin Id, the mammalian homolog of *Drosophila Myo31DF*, has been reported to be expressed in neurons, whereas its subcellular localization in neurons remained unknown. Here, we investigated the subcellular localization of myosin Id and determined the domain responsible for it. We found that myosin Id is enriched in the F-actin-rich pseudopodia of HEK293T cells and in the dendritic spines of primary hippocampal neurons. Both deletion and substitution of the tail homology 1 (TH1) domain drastically diminishes its colocalization with F-actin. In addition, the mutant form lacking the TH1 domain is less distributed in dendritic spines than is the full-length form. Taken together, our findings reveal that myosin Id localizes in dendritic spines through the TH1 domain.

Keywords

Dendritic spine; Actin filament; Myosin Id; Tail homology 1 domain; Primary hippocampal neuron

Introduction

Dendritic spines are postsynaptic compartments that receive excitatory neurotransmitters, such as glutamate, released from the presynaptic terminals. The changing in the shape and size of dendritic spines in response to environmental stimuli is an essential process for synaptic plasticity (Caroni et al., 2012). The actin cytoskeleton is a major component of dendritic spines and plays a critical role in their structural dynamics (Cingolani and Goda, 2008; Hotulainen and Hoogenraad, 2010). In addition, a variety of actin-binding proteins such as Arp2/3 (Spence et al., 2016), ADF/cofilin (Gu et al., 2010), and myosins (Rex et al., 2010; Ryu et al., 2006) are involved in regulation of dendritic spine morphology. The importance of understanding the regulatory mechanisms underlying the dynamics of dendritic spines has been increasingly emphasized because abnormal spine morphology is associated with neurodevelopmental disorders such as autism spectrum disorder (ASD) and schizophrenia (Dölen et al., 2007; Penzes et al., 2011).

Myosins are motor proteins that move along actin filaments by using the energy of ATP hydrolysis (Kneussel and Wagner, 2013). Myosins form a large family that consists of approximately 40 members. Of these, class I myosins (myosin Ia –Ih) are monomeric proteins that carry three different domains in common, namely an N-terminal motor domain, a neck domain, and a C-terminal tail homology 1 (TH1) domain (McConnell and Tyska, 2010; McIntosh and Ostap, 2016). The motor

domain contains ATPase and an actin-binding site. The TH1 domain is capable of binding to anionic phospholipids. The neck domain resides between the former two domains and contains IQ motifs that bind to calmodulin. Subcellular localization of myosin I isoforms has been assumed to be determined by its affinity to actin or phospholipids. In fact, class I myosins act as a linker between actin filaments and the plasma membrane in a variety of cell types (Bose et al., 2004; Komaba and Coluccio, 2010; Patino-Lopez et al., 2010; Tyska and Mooseker, 2002).

The tendency of class I myosins to localize actin-rich protrusions prompted us to hypothesize that they are enriched in actin-rich dendritic spines. In particular, myosin Id is a promising candidate because it is expressed in neurons (Benesh et al., 2012). In addition, a linkage analysis suggesting that myosin Id is a potential risk gene for ASD (Stone et al., 2007) implied that myosin Id might play an important role in dendritic spines. Myosin Id is a homolog of *Drosophila* myosin IA (encoded by *Myo31DF*), which is essential for the left-right visceral asymmetry of *Drosophila* organs (Hozumi et al., 2006). In mammals, myosin Id is highly enriched in the microvilli of intestinal epithelial cells (Benesh et al., 2010). However, its subcellular localization in neurons remained unknown.

Here, we showed that myosin Id localizes in the dendritic spines of primary hippocampal neurons. We also found that the TH1 domain is critical for its distribution in dendritic spines.

Materials and Methods

Mice

All experiments using CD1 and C57BL/6J mice were carried out according to the Guide for the Care and Use of Laboratory Animals at the University of Tsukuba.

DNA constructs

The open reading frame of the myosin Id gene was amplified from mouse brain cDNA using PCR and subcloned into a pEGFP-C1 vector (Clontech) so that EGFP was fused to its N-terminus. Mutant vectors lacking the conserved sequence corresponding to the actin-binding site of *Drosophila* homolog myosin IA (Δ584–594) (Morgan et al., 1994), the TH1 domain (ΔTH1), or the motor domain (IQ + TH1) and mutant vectors in which each of the "signature basic residues" in the TH1 domain is substituted with alanine (K865A, R875A) (Hokanson and Ostap, 2006) were prepared using a PrimeSTAR Mutagenesis Basal Kit (TaKaRa).

Cell cultures and transfection

Primary hippocampal neurons were prepared from mouse embryos at embryonic day 16.5. Briefly, the hippocampi were dissected and digested with 0.25% trypsin/HBSS for 15 minutes at 37 °C. The

cells were dissociated by gentle pipetting and plated at a density of 8×10^4 cells on 12-well plates. In advance, coverslips were placed on the well and coated with 0.04% polyethylenimine and 1 mg/ml poly-L-lysine. Primary hippocampal neurons were maintained in MEM supplemented with 6 g/l glucose, 1 mM sodium pyruvate, 2 mM GlutaMax (Gibco), and 2% NeuroBrew-21 (Miltenyi Biotec). HEK293T cells were cultured in DMEM supplemented with 10% heat-inactivated fetal bovine serum and 1% Pen Strep (Gibco). Both groups of cells were transfected with vectors using Lipofectamine 2000 (Invitrogen).

Quantitative RT-PCR

Total RNA was extracted from mouse brains and primary hippocampal neurons using NucleoSpin RNA (Macherey-Nagel) and cDNA was synthesized using a High-Capacity RNA-to-cDNA Kit (Applied Biosystems) according to the manufacturer's instructions. Real-time PCR was performed on an Eco Real-time PCR System (Illumina) with THUNDERBIRD SYBR qPCR Mix (Toyobo). The analyses were performed in duplicate. Relative expression levels were calculated with the $2^{-\Delta\Delta Ct}$ method using HPRT as an internal control. The primers used were as follows: Myosin Id forward, ATTCGAACACCCCGTACACT-3'; Myosin Id reverse, 5'-TTGGTCCTCTTGTACCGCAT-3'; HPRT forward, 5'-TTGTTGTTGGATATGCCCTTGACTA-3'; and HPRT reverse,

5’-AGGCAGATGGCCACAGGACTA-3’.

Immunoblot analysis

To obtain a synaptosomal fraction, adult mouse cerebra were homogenized in ice-cold TEVP buffer (10 mM Tris, pH 7.5, 1 mM EDTA, 1 mM EGTA, 320 mM sucrose) containing a cOmplete Protease Inhibitor Cocktail (Roche) and were centrifuged at 1000 × g for 10 minutes at 4 °C to remove nuclei and large debris. The supernatant (S1) was centrifuged at 10,000 × g for 20 minutes at 4 °C. The resulting supernatant (S2) was collected as a cytoplasmic faction, and the remaining pellet (P2), a crude synaptosomal fraction, was solubilized with 1% SDS in TEVP buffer. HEK293T cells were lysed with RIPA buffer (50 mM Tris, pH 8.0, 150 mM NaCl, 1% Triton X-100, 0.1% SDS) containing the protease inhibitors.

The lysates were mixed with Laemmli sample buffer (Bio-Rad) and heated for 3 minutes at 95°C. The samples were electrophoresed by SDS-PAGE and transferred to PVDF membranes. The membranes were blocked with 5% skim milk in TBS-0.05% Tween-20 for 30 minutes at room temperature and incubated with primary antibodies overnight at 4 °C. The antibodies used were as follows: anti-GFP (1:1000, A11122; Invitrogen), anti-myosin Id (1:200, sc-66982, Santa Cruz Biotechnology), anti-PSD-95 (1:2000, ab13552; Abcam) and anti-β-actin (1:5000, A5441, Sigma).

The following day, HRP-linked secondary antibodies (1:10,000, Cell Signaling Technology) and Immobilon HRP Chemiluminescence HRP substrate (Millipore) were used for detection. The bands were visualized with a C-DiGit Blot Scanner (LI-COR Bioscience) and quantified with Image Studio Digits software (LI-COR Bioscience). The signal intensity of each sample was normalized to that of β-actin.

Immunocytochemistry

The cells on coverslips were fixed with 4% paraformaldehyde in PBS for 15 minutes at room temperature. The cells were then permeabilized and blocked with 3% normal goat serum plus 0.1% Triton X-100 in PBS for 1 hour at room temperature and incubated with primary antibodies overnight at 4 °C. The antibodies used were as follows: anti-myosin Id (1:200, sc-66982, Santa Cruz Biotechnology) and anti-PSD-95 (1:2000, ab13552; Abcam). The following day, the cells were washed with PBS-0.05% Tween-20 and then incubated with Alexa Fluor 568-conjugated secondary antibody (Molecular Probes) for 1 hour at room temperature. For F-actin staining, the cells were incubated with Alexa Fluor 568-phalloidin (Molecular Probes) for 30 minutes at room temperature. The coverslips were mounted onto glass slides using a mounting medium.

Image analysis

Fluorescence images were acquired on a LSM510 laser confocal microscope (Carl Zeiss) with a 40×/1.2 NA water-immersion objective and analyzed with Image J software (NIH). Each area of interest was enclosed manually and its fluorescence intensity was quantified. The areas of pseudopodia were determined based on F-actin accumulation. The areas of cytoplasm were enclosed except for pseudopodia and nuclei. The areas of dendritic spines were determined based on the morphology visualized by mCherry (Hotulainen and Hoogenraad, 2010).

Statistical analysis

All data are expressed as means ± SEMs. Differences between the two groups were analyzed using a Student *t* test. For comparison within the same samples, a paired *t* test was applied. For multiple comparisons, the Tukey Honest Significant Differences (HSD) test or the Dunnett test was applied. All statistical analyses were performed using R software (http://www.r-project.org). Probability values less than 0.05 were considered significant.

Results

Myosin Id is enriched in the synaptosomal fraction of mouse brain.

151 It has already been reported that myosin Id is expressed in neurons (Benesh et al., 2012). To test
152 whether there is a regional preference for its expression within the brain, we collected RNA from
153 different subregions of the mouse brain and analyzed myosin Id mRNA expression using qRT-PCR.
154 We found that myosin Id was expressed throughout the mouse brain, but it was more highly
155 expressed in the striatum, thalamus, and brain stem (Fig. 1A). Next, we examined myosin Id mRNA
156 expression in the whole brain at different ages. At P28, the young adult stage, it was expressed twice
157 as much as at P0 (Fig. 1B). Notably, oligodendrocytes also express myosin Id (Yamazaki et al., 2014).
158 The upregulation of myosin Id at P28 could be attributed to postnatal proliferation of
159 oligodendrocytes. Thus, we prepared primary hippocampal neurons to minimize the effect of
160 oligodendrocytes. As a result, myosin Id mRNA levels were unchanged between days *in vitro* (DIV)
161 1, 7, and 14 (Fig. 1C). Furthermore, to investigate the localization of myosin Id protein, we prepared
162 synaptosomal and cytoplasmic fractions from adult mouse cerebra. Immunoblot analysis with
163 anti-myosin Id antibody has revealed that myosin Id protein is significantly enriched in the
164 synaptosomal fraction compared to the cytoplasmic fraction (Fig. 1D, E) in a similar manner to
165 PSD-95, a well-known postsynaptic marker. These data suggest that myosin Id is a synapse-related
166 molecule.
167

Myosin Id localizes in the F-actin-rich pseudopodia of HEK293T cells.

To characterize the subcellular localization of myosin Id protein, we prepared an expression vector that produces EGFP-tagged myosin Id protein. We transfected HEK293T cells with this vector and confirmed successful expression of EGFP-myosin Id protein as shown by immunoblot analysis (Fig. 2A). In addition, immunocytochemical analyses showed that the GFP signals were highly enriched in the F-actin-rich pseudopodia (Fig. 2B).

Myosin Id localizes in the dendritic spines of primary hippocampal neurons.

Given that dendritic spines are rich in the actin cytoskeleton (Cingolani and Goda, 2008), we tested whether myosin Id accumulates there. We transfected primary hippocampal neurons at DIV13, when the dendritic spines are formed, with an EGFP-myosin Id vector. An mCherry-C1 vector was co-transfected as a reference. At 24 hours after transfection, we examined the fluorescence intensities of both EGFP and mCherry at the same spine. The spine/shaft ratio of GFP was statistically higher than that of mCherry at the same spine (Fig. 3A, B), which demonstrated that myosin Id is enriched in dendritic spines. Consistent with this, GFP fluorescence in the PSD-95-positive puncta (dendritic spines) was significantly higher than that in the neighboring PSD-95-negative shafts (Fig. 3C, D). These results reveal that myosin Id protein localizes in dendritic spines.

185

186 *Deletion of the TH1 domain drastically diminishes its colocalization with F-actin in the*

187 *pseudopodia.*

188 To identify a region responsible for its localization, we created mutant vectors lacking specific

189 regions (Fig. 4A). To search for a possible actin-binding site, we identified the conserved sequence

190 (residues 584–594) corresponding to the actin-binding site of *Drosophila* homolog myosin IA

191 (Morgan et al., 1994). Deletion of residues 584–594 (Δ584–594) reduced its accumulation in the

192 F-actin-rich pseudopodia, yet the reduction was marginal (Fig. 4B, C). Surprisingly, deletion of the

193 TH1 domain (ΔTH1) drastically diminished its accumulation in the pseudopodia. A C-terminal

194 fragment consisting of the IQ motifs and the TH1 domain (IQ + TH1) localized mainly in the nuclei.

195 This nuclear localization is similar to the findings of a previous study with myosin Ig (Patino-Lopez

196 et al., 2010), which has higher homology to myosin Id (59%, ClastalW;

197 http://www.genome.jp/tools-bin/clustalw) than do any other class I myosins (29−37%). Deletion of

198 the N-terminal portion might unmask a cryptic nuclear localization signal. Notably, the IQ + TH1

199 fragment was also enriched in the pseudopodia.

200

201 *"Signature basic residues" in the TH1 domain are critical for its colocalization with F-actin.*

202 The TH1 domain in class I myosins commonly includes the pleckstrin homology (PH) domain,
203 which is capable of binding to phospholipids (McConnell and Tyska, 2010). A previous study with
204 myosin Ic determined the conserved basic residues ("signature basic residues") that are critical for its
205 binding capacity (Hokanson et al., 2006). We created two additional mutant vectors of myosin Id in
206 which each of the corresponding basic residues is substituted with alanine (K865A or R875A).
207 Notably, both of the mutant forms displayed diminished colocalization with F-actin in the
208 pseudopodia (Fig 5A, B). These results reveal that the TH1 domain is critical for its colocalization
209 with F-actin.
210
211 *The TH1 domain is critical for distribution of myosin Id from the soma to the dendrites and for its*
212 *enrichment in dendritic spines.*
213 To test whether the TH1 domain is important for localization of myosin Id even in neurons, we
214 transfected primary hippocampal neurons at DIV13 with full-length or ΔTH1 vectors. Notably, the
215 ΔTH1 fragment was less distributed from the soma to the dendrites than was full-length myosin Id
216 (Fig. 6A, B). In addition, the ΔTH1 fragment showed diminished accumulation in dendritic spines as
217 evidenced by reduction in the GFP fluorescence ratio of the spines to the shafts (Fig. 6C, D). These
218 results suggest that the TH1 domain is critical for the distribution of myosin Id from the soma to the

219 dendrites and for its enrichment in dendritic spines.

220

221 **Discussion**

222 In this study, we have revealed that myosin Id localizes in the dendritic spines of neurons. Domain
223 analysis suggested that the TH1 domain is critical for distribution of myosin Id in dendritic spines.
224 To our knowledge, ours is the first study to describe the subcellular localization of myosin Id in
225 neurons.

226 Fine-tuning of synaptic transmission in accordance with environmental stimuli, namely synaptic
227 plasticity, underlies brain functions such as learning and memory. A number of molecules in dendritic
228 spines are involved in regulation of synaptic plasticity (Caroni et al., 2012; Koleske, 2013).
229 Abnormalities in synaptic transmission have been proposed to underlie the pathogenesis of ASD
230 (Barak and Feng, 2016). Clinical studies have shown that individuals with ASD exhibit a higher
231 density of dendritic spines than do age-matched controls (Penzes et al., 2011). In addition,
232 *Fmr1*-knockout mice, a model for fragile X syndrome, exhibit enhanced mGluR5-dependent
233 long-term depression accompanied by a higher density of dendritic spines in the hippocampi (Dölen
234 et al., 2007; Huber et al., 2002). These studies highlighted the importance of understanding the
235 regulatory mechanisms underlying the dynamics of dendritic spines. Combined with the linkage

236 analysis suggesting myosin Id as a potential risk gene for ASD (Stone et al., 2007), our results
237 showing that myosin Id is enriched in dendritic spines raise the possibility that myosin Id regulates
238 synaptic transmission in dendritic spines and, furthermore, that its dysfunction would result in ASD.
239 Further analyses such as by means of electrophysiological and behavioral experiments will be
240 required to test this possibility.

241 In this study, both deletion and substitution of the TH1 domain drastically diminished its
242 enrichment in the F-actin-rich pseudopodia. Although the TH1 domain includes the PH domain,
243 which is capable of binding to anionic phospholipids (Hokanson et al., 2006), it is unlikely that its
244 binding to phospholipids solely determines the localization of myosin Id because the GFP signals did
245 not accumulate on the plasma membrane. Unexpectedly, deletion of the conserved domain
246 corresponding to the actin-binding site in *Drosophila* homolog myosin IA (Morgan et al., 1994)
247 resulted in marginal reduction of the enrichment in pseudopodia. These results indicate that this
248 conserved domain is not critical for its actin binding and, furthermore, that actin-binding sites in the
249 motor domain of mammalian myosin Id remain unclear. Interestingly, our study suggests that the
250 TH1 domain critically mediates binding of mammalian myosin Id to F-actin. Previous studies
251 showing that the PH domain interacts with F-actin (Macia et al., 2008; Yao et al., 1999) support our
252 results. Further biophysical and biochemical studies will be required to clarify how myosin Id

interacts with actin filaments.

Neurons have a specialized transport system to deliver dendritic molecules efficiently throughout the multiple and highly branched dendrites. For this delivery, neurons use motor proteins, that is, kinesins, dyneins, and myosins. These motor proteins carry their cargo to the destination by moving along cytoskeletons (microtubules or actin filaments) (Hirokawa et al., 2010). Actin filaments exist not only in the dendritic spines but also in the dendritic shafts as long bundles (Konietzny et al., 2017). Previous studies have shown that an actin-depolymerizing factor, cytochalasin D, disturbs the dendritic localization of some specific molecules (Balasanyan and Arnold, 2014; Lewis et al., 2009), which suggests that actin filaments offer some paths for dendritic transport. In those previous studies, myosin Va was suggested as a carrier in this actin-based dendritic transport. In our study, the ΔTH1 were less distributed from the soma to the dendrites than was the full-length form. Combined with the fact that ΔTH1 is defective in binding to F-actin, it could be assumed that myosin Id moves to the dendrites along actin filaments through the TH1 domain by its own energy. However, it cannot be ruled out that myosin Id is transported to dendrites by different molecules. Additional analysis of a mutant form with defective ATPase activity that cannot use the energy of ATP would provide us with useful information.

At present, the function of myosin Id in neurons remains to be uncovered. In a variety of cell types,

class I myosins work as a linker between actin filaments and phospholipids (McIntosh and Ostap, 2016). In fact, class I myosins prefer to localize actin-rich protrusions such as the microvilli of enterocytes (myosins Ia and Id) (Tyska et al., 2005; Tyska and Mooseker, 2004), stereocilia of auditory hair cells (myosin Ic) (Holt et al., 2002), and foot processes of podocytes (myosin Ie) (Mele et al., 2011), where they are involved in maintenance of membrane tension. In addition, class I myosins have been proposed to dock or tether vesicles to the plasma membrane (Boguslavsky et al., 2012). If myosin Id shares these functions, it could be possible that myosin Id modulates synaptic transmission by regulating dendritic spine architecture or vesicular transport.

In conclusion, myosin Id, a member of the class I myosins, localizes in dendritic spines through the TH1 domain. Our study also provides the possibility that the TH1 domain, rather than the motor domain, includes a critical actin-binding site in myosin Id.

Author contributions

R.K. and Y.T. designed the experiments. R.K. and S.T. performed the experiments. R.K. analyzed the data and wrote the manuscript.

Conflicts of interest

The authors declare no competing financial interests.

Acknowledgements

We thank Masae Ohtsuka for technical assistance and Flaminia Miyamasu for English revision. This work was primarily supported by the University of Tsukuba Basic Research Support Program Type A (R.K.) and was partly supported by the Brain Mapping by Integrated Neurotechnologies for Disease Studies (Brain/MINDS) from the Japan Agency for Medical Research and Development (AMED) under Grant Number JP17dm0207047 (Y.T.) and by a grant from the Uehara Memorial Foundation (Y.T.).

References

Balasanyan, V., Arnold, D.B., 2014. Actin and myosin-dependent localization of mRNA to dendrites. PLoS One 9. https://doi.org/10.1371/journal.pone.0092349

Barak, B., Feng, G., 2016. Neurobiology of social behavior abnormalities in autism and Williams syndrome. Nat. Neurosci. 19, 647–655. https://doi.org/10.1038/nn.4276

Benesh, A.E., Fleming, J.T., Chiang, C., Carter, B.D., Tyska, M.J., 2012. Expression and localization

of myosin-1d in the developing nervous system. Brain Res. 1440, 9–22. https://doi.org/10.1016/j.brainres.2011.12.054

Benesh, A.E., Nambiar, R., McConnell, R.E., Mao, S., Tabb, D.L., Tyska, M.J., 2010. Differential Localization and Dynamics of Class I Myosins in the Enterocyte Microvillus. Mol. Biol. Cell 21, 970–978. https://doi.org/10.1091/mbc.E09-07-0638

Boguslavsky, S., Chiu, T., Foley, K.P., Osorio-Fuentealba, C., Antonescu, C.N., Bayer, K.U., Bilan, P.J., Klip, A., 2012. Myo1c binding to submembrane actin mediates insulin-induced tethering of GLUT4 vesicles. Mol. Biol. Cell 23, 4065–4078. https://doi.org/10.1091/mbc.E12-04-0263

Bose, A., Robida, S., Furcinitti, P.S., Chawla, A., Fogarty, K., Corvera, S., Czech, M.P., 2004. Unconventional myosin Myo1c promotes membrane fusion in a regulated exocytic pathway. Mol. Cell. Biol. 24, 5447–5458. https://doi.org/10.1128/MCB.24.12.5447-5458.2004

Caroni, P., Donato, F., Muller, D., 2012. Structural plasticity upon learning: Regulation and functions. Nat. Rev. Neurosci. 13, 478–490. https://doi.org/10.1038/nrn3258

Cingolani, L.A., Goda, Y., 2008. Actin in action: The interplay between the actin cytoskeleton and synaptic efficacy. Nat. Rev. Neurosci. 9, 344–356. https://doi.org/10.1038/nrn2373

Dölen, G., Osterweil, E., Rao, B.S.S., Smith, G.B., Auerbach, B.D., Chattarji, S., Bear, M.F., 2007. Correction of Fragile X Syndrome in Mice. Neuron 56, 955–962.

https://doi.org/10.1016/j.neuron.2007.12.001

Gu, J., Lee, C.W., Fan, Y., Komlos, D., Tang, X., Sun, C., Yu, K., Hartzell, H.C., Chen, G., Bamburg, J.R., Zheng, J.Q., 2010. ADF/cofilin-mediated actin dynamics regulate AMPA receptor trafficking during synaptic plasticity. Nat. Neurosci. 13, 1208–1215. https://doi.org/10.1038/nn.2634

Hirokawa, N., Niwa, S., Tanaka, Y., 2010. Molecular motors in neurons: Transport mechanisms and roles in brain function, development, and disease. Neuron 68, 610–638. https://doi.org/10.1016/j.neuron.2010.09.039

Hokanson, D.E., Laakso, J.M., Lin, T., Sept, D., Ostap, E.M., 2006. Myo1c Binds Phosphoinositides through a Putative Pleckstrin Homology Domain. Mol. Biol. Cell 17, 4856–4865. https://doi.org/10.1091/mbc.E06-05-0449

Hokanson, D.E., Ostap, E.M., 2006. Myo1c binds tightly and specifically to phosphatidylinositol 4,5-bisphosphate and inositol 1,4,5-trisphosphate. Proc. Natl. Acad. Sci. U. S. A. 103, 3118–3123. https://doi.org/10.1073/pnas.0505685103

Holt, J.R., Gillespie, S.K.H., Provance, D.W., Shah, K., Shokat, K.M., Corey, D.P., Mercer, J.A., Gillespie, P.G., 2002. A chemical-genetic strategy implicates myosin-1c in adaptation by hair cells. Cell 108, 371–381. https://doi.org/10.1016/S0092-8674(02)00629-3

338 Hotulainen, P., Hoogenraad, C.C., 2010. Actin in dendritic spines: Connecting dynamics to function.
339 J. Cell Biol. 189, 619–629. https://doi.org/10.1083/jcb.201003008
340 Hozumi, S., Maeda, R., Taniguchi, K., Kanai, M., Shirakabe, S., Sasamura, T., Spéder, P., Noselli, S.,
341 Aigaki, T., Murakami, R., Matsuno, K., 2006. An unconventional myosin in Drosophila
342 reverses the default handedness in visceral organs. Nature 440, 798–802.
343 https://doi.org/10.1038/nature04625
344 Huber, K.M., Gallagher, S.M., Warren, S.T., Bear, M.F., 2002. Altered synaptic plasticity in a mouse
345 model of fragile X mental retardation. Proc. Natl. Acad. Sci. 99, 7746–7750.
346 https://doi.org/10.1073/pnas.122205699
347 Kneussel, M., Wagner, W., 2013. Myosin motors at neuronal synapses: Drivers of membrane
348 transport and actin dynamics. Nat. Rev. Neurosci. 14, 233–247. https://doi.org/10.1038/nrn3445
349 Koleske, A.J., 2013. Molecular mechanisms of dendrite stability. Nat. Rev. Neurosci. 14, 536–550.
350 https://doi.org/10.1038/nrn3486
351 Komaba, S., Coluccio, L.M., 2010. Localization of myosin 1b to actin protrusions requires
352 phosphoinositide binding. J. Biol. Chem. 285, 27686–27693.
353 https://doi.org/10.1074/jbc.M109.087270
354 Konietzny, A., Bär, J., Mikhaylova, M., 2017. Dendritic Actin Cytoskeleton: Structure, Functions,

and Regulations. Front. Cell. Neurosci. 11, 1–10. https://doi.org/10.3389/fncel.2017.00147

Lewis, T.L., Mao, T., Svoboda, K., Arnold, D.B., 2009. Myosin-dependent targeting of transmembrane proteins to neuronal dendrites. Nat. Neurosci. 12, 568–576. https://doi.org/10.1038/nn.2318

Macia, E., Partisani, M., Favard, C., Mortier, E., Zimmermann, P., Carlier, M.F., Gounon, P., Luton, F., Franco, M., 2008. The pleckstrin homology domain of the Arf6-specific exchange factor EFA6 localizes to the plasma membrane by interacting with phosphatidylinositol 4,5-bisphosphate and F-actin. J. Biol. Chem. 283, 19836–19844. https://doi.org/10.1074/jbc.M800781200

McConnell, R.E., Tyska, M.J., 2010. Leveraging the membrane - cytoskeleton interface with myosin-1. Trends Cell Biol. 20, 418–426. https://doi.org/10.1016/j.tcb.2010.04.004

McIntosh, B.B., Ostap, E.M., 2016. Myosin-I molecular motors at a glance. J. Cell Sci. 129, 2689–2695. https://doi.org/10.1242/jcs.186403

Mele, C., Iatropoulos, P., Donadelli, R., Calabria, A., Maranta, R., Cassis, P., Buelli, S., Tomasoni, S., Piras, R., Krendel, M., Bettoni, S., Morigi, M., Delledonne, M., Pecoraro, C., Abbate, I., Capobianchi, M.R., Hildebrandt, F., Otto, E., Schaefer, F., Macciardi, F., Ozaltin, F., Emre, S., Ibsirlioglu, T., Benigni, A., Remuzzi, G., Noris, M., 2011. MYO1E Mutations and Childhood

372 Familial Focal Segmental Glomerulosclerosis. N. Engl. J. Med. 365, 295–306.
373 https://doi.org/10.1056/NEJMoa1101273
374 Morgan, N.S., Skovronsky, D.M., Artavanis-Tsakonas, S., Mooseker, M.S., 1994. The Molecular
375 Cloning and Characterization of Drosophila melanogaster Myosin-IA and Myosin-IB. J. Mol.
376 Biol. 239, 347–356. https://doi.org/10.1006/jmbi.1994.1376
377 Patino-Lopez, G., Aravind, L., Dong, X., Kruhlak, M.J., Ostap, E.M., Shaw, S., 2010. Myosin 1G is
378 an abundant class I myosin in lymphocytes whose localization at the plasma membrane depends
379 on its ancient divergent pleckstrin homology (PH) domain (Myo1PH). J. Biol. Chem. 285,
380 8675–8686. https://doi.org/10.1074/jbc.M109.086959
381 Penzes, P., Cahill, M.E., Jones, K.A., Vanleeuwen, J.E., Woolfrey, K.M., 2011. Dendritic spine
382 pathology in neuropsychiatric disorders. Nat. Neurosci. 14, 285–293.
383 https://doi.org/10.1038/nn.2741
384 Rex, C.S., Gavin, C.F., Rubio, M.D., Kramar, E.A., Chen, L.Y., Jia, Y., Huganir, R.L., Muzyczka,
385 N., Gall, C.M., Miller, C.A., Lynch, G., Rumbaugh, G., 2010. Myosin IIb Regulates actin
386 dynamics during synaptic plasticity and memory formation. Neuron 67, 603–617.
387 https://doi.org/10.1016/j.neuron.2010.07.016
388 Ryu, J., Liu, L., Wong, T.P., Wu, D.C., Burette, A., Weinberg, R., Wang, Y.T., Sheng, M., 2006. A

critical role for myosin IIB in dendritic spine morphology and synaptic function. Neuron 49, 175–182. https://doi.org/10.1016/j.neuron.2005.12.017

Spence, E.F., Kanak, D.J., Carlson, B.R., Soderling, S.H., 2016. The Arp2/3 Complex Is Essential for Distinct Stages of Spine Synapse Maturation, Including Synapse Unsilencing. J. Neurosci. 36, 9696–9709. https://doi.org/10.1523/JNEUROSCI.0876-16.2016

Stone, J.L., Merriman, B., Cantor, R.M., Geschwind, D.H., Nelson, S.F., 2007. High density SNP association study of a major autism linkage region on chromosome 17. Hum. Mol. Genet. 16, 704–715. https://doi.org/10.1093/hmg/ddm015

Tyska, M.J., Mackey, A.T., Huang, J.-D., Copeland, N.G., Jenkins, N.A., Mooseker, and M.S., 2005. Myosin-1a Is Critical for Normal Brush Border Structure and Composition. Mol. Biol. Cell 16, 2443–2457. https://doi.org/10.1091/mbc.E04-12-1116

Tyska, M.J., Mooseker, M.S., 2004. A role for myosin-1A in the localization of a brush border disaccharidase. J. Cell Biol. 165, 395–405. https://doi.org/10.1083/jcb.200310031

Tyska, M.J., Mooseker, M.S., 2002. MYO1A (brush border myosin I) dynamics in the brush border of LLC-PK1-CL4 cells. Biophys. J. 82, 1869–1883. https://doi.org/10.1016/S0006-3495(02)75537-9

Yamazaki, R., Ishibashi, T., Baba, H., Yamaguchi, Y., 2014. Unconventional myosin ID is expressed

406 in myelinating oligodendrocytes. J. Neurosci. Res. 92, 1286–1294.
407 https://doi.org/10.1002/jnr.23419
408 Yao, L., Janmey, P., Frigeri, L.G., Han, W., Fujita, J., Kawakami, Y., Apgar, J.R., Kawakami, T.,
409 1999. Pleckstrin homology domains interact with filamentous actin. J. Biol. Chem. 274, 19752–
410 19761. https://doi.org/10.1074/jbc.274.28.19752
411

Figure legends

Fig. 1. Myosin Id is enriched in the synaptosomal fraction of mouse brain. (A) qRT-PCR analysis for myosin Id mRNA in the subregions of mouse brain at 8 weeks of age. n = 4 per group. Data are expressed relative to the mean value of all samples. (B) Myosin Id mRNA expression in the whole brain during postnatal development. n = 4 per each group. Data are expressed relative to the P0. *$p <$ 0.05, Dunnett multiple comparison test (vs P0). (C) Myosin Id mRNA expression in primary hippocampal neurons at different days *in vitro* (DIV). Data are expressed relative to the DIV 1. n = 3 per group. (D) Immunoblot analysis of cytoplasmic and synaptosomal fractions prepared from adult mouse cerebra. Myosin Id protein is significantly enriched in the synaptosomal fraction. PSD-95 is a postsynaptic marker. (E) Signal intensity of the immunoblot analysis. Data are expressed as a ratio to β-actin. n = 3 cerebra. *$p < 0.05$, paired *t* test.

Fig. 2. Myosin Id localizes in the F-actin-rich pseudopodia of HEK293T cells. (A) Immunoblot analysis for EGFP-myosin Id expression by HEK293T. Anti-GFP antibody was used as the primary antibody. A band of EGFP-myosin Id protein appears at approximately 150 kDa (arrow). (B) Confocal images of HEK293T cells at 24 hours after transfection. EGFP-myosin Id (green) was overlapped with F-actin (red) in the pseudopodia (arrowheads). Scale bar: 20 μm.

Fig. 3. Myosin Id localizes in the dendritic spines of primary hippocampal neurons. (A) Confocal images of primary hippocampal neurons at DIV14 transfected with both EGFP-myosin Id (green) and mCherry (red), which was used as a reference. The lower panels show higher magnification images of the square areas in the upper panels. The yellow and white circles indicate the areas of the spines and the neighboring shafts, respectively. Scale bars: upper panels, 50 μm; lower panels, 5 μm. (B) A scatterplot representing the fluorescence ratio of the spines to the shafts. GFP fluorescence (y-axis) is biased to the spine as evidenced by its significantly higher fluorescence ratio than that of mCherry (x-axis) at the same spines. n = 79 spines (6 neurons). $p < 0.05$, paired *t* test. (C) EGFP-myosin Id (green) colocalizes with PSD-95 (red), a postsynaptic marker. Scale bar: 5 μm. (D) GFP fluorescence in the PSD-95-positive puncta (spines) is significantly higher than that in the neighboring PSD-95-negative shafts. n = 77 puncta (4 neurons). $*p < 0.05$, paired *t* test.

Fig. 4. Deletion of the TH1 domain drastically diminishes its colocalization with F-actin in the pseudopodia. (A) Schematic protein structures of full-length and mutant forms of myosin Id. The conserved region (residues 584−594) corresponding to the actin-binding site of *Drosophila* homolog myosin IA (Δ584−594), the TH1 domain (ΔTH1), or the motor domain (IQ + TH1) was deleted in

each mutant vector. (B) Confocal images of HEK293T cells transfected with full-length or mutant forms of myosin Id. Scale bar: 20 μm. Arrowheads indicate the F-actin-rich pseudopodia (red). (C) GFP fluorescence ratio of pseudopodia to cytoplasm. n = 10–12 cells per group. *$p < 0.05$, **$p < 0.01$, ***$p < 0.001$, Tukey HSD test.

Fig. 5. "Signature basic residues" in the TH1 domain are critical for its colocalization with F-actin. (A) Confocal images of HEK293T cells transfected with full-length or mutant forms in which each of the "signature basic residues" was substituted with alanine (K865A, R875A). Scale bar: 20 μm. (B) GFP fluorescence ratio of pseudopodia to cytoplasm. n = 10 cells per group. * $p < 0.05$, Tukey HSD test.

Fig. 6. The TH1 domain is critical for distribution of myosin Id from the soma to the dendrites and for its enrichment in the dendritic spines of primary hippocampal neurons. (A) Primary hippocampal neurons at DIV14 transfected with full-length myosin Id or ΔTH1 vectors. Scale bar: 50 μm. (B) GFP fluorescence ratio of dendrites to nuclei. n = 6 neurons per group. *$p < 0.05$, Student *t* test. (C) Confocal images of dendritic spines. Scale bar: 5 μm. (D) GFP fluorescence ratio of spines to shafts. mCherry fluorescence was used as a reference. n = 90 (full-length) or 91 (ΔTH1) spines from 4

463 neurons per group. *$p < 0.05$, Student *t* test.

Koshida et al., Fig 1.

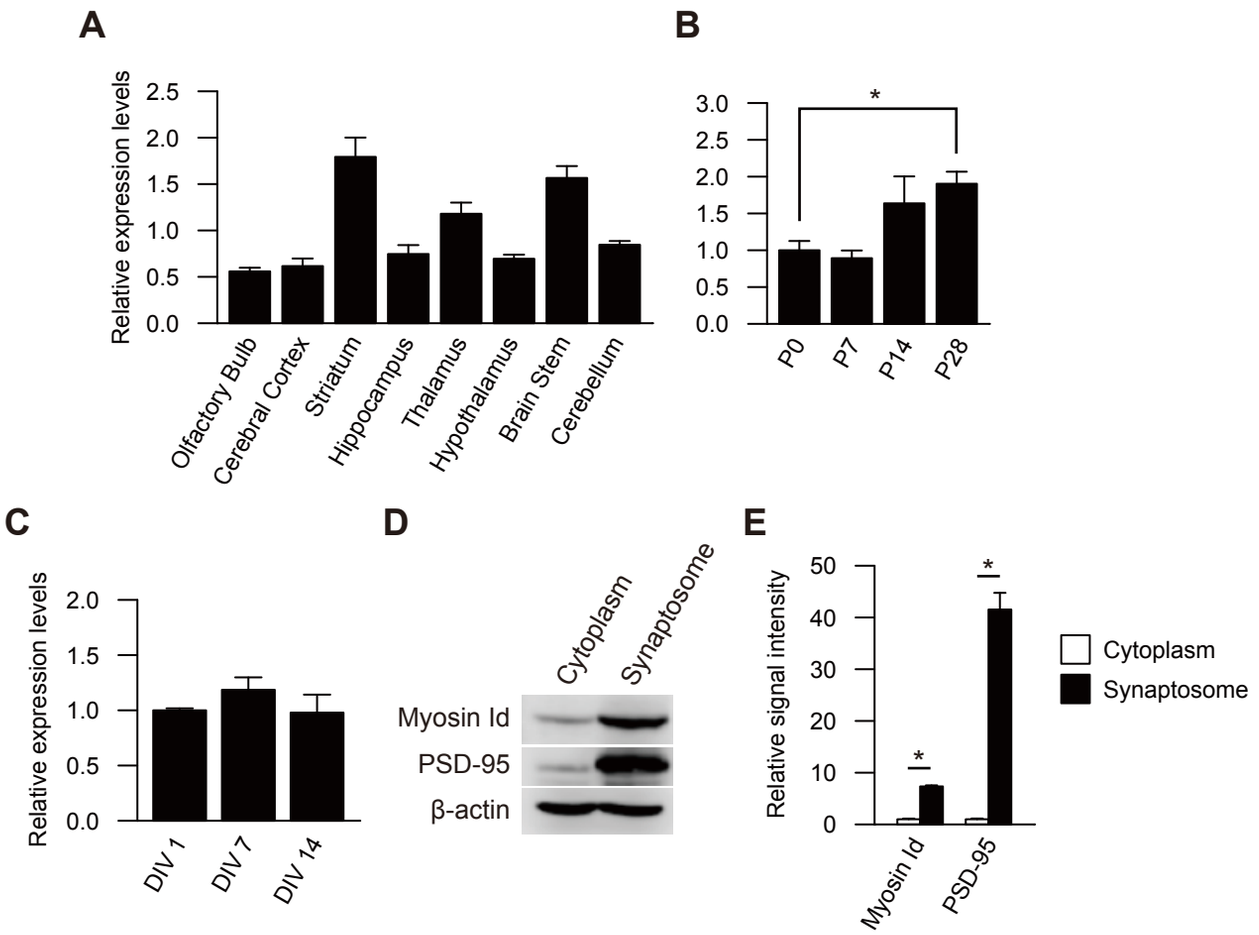

Koshida et al., Fig 2.

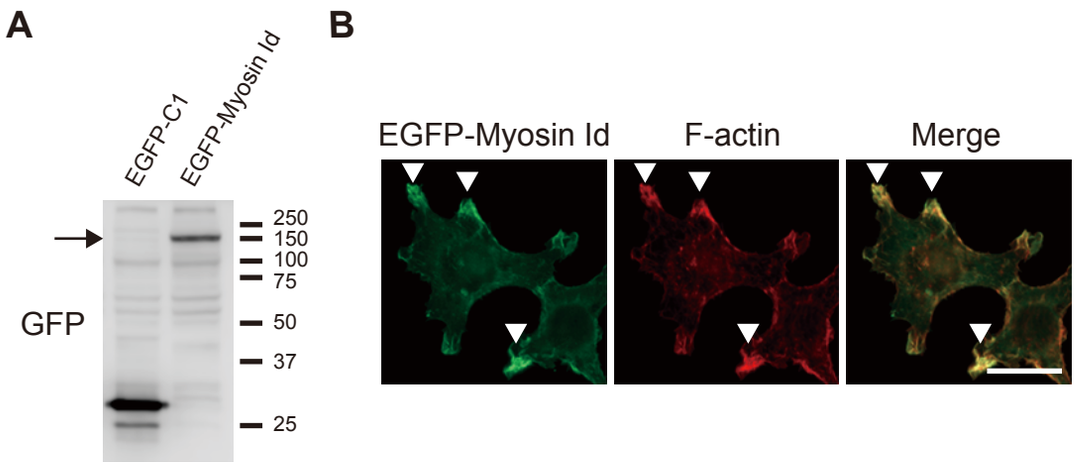

Koshida et al., Fig 3.

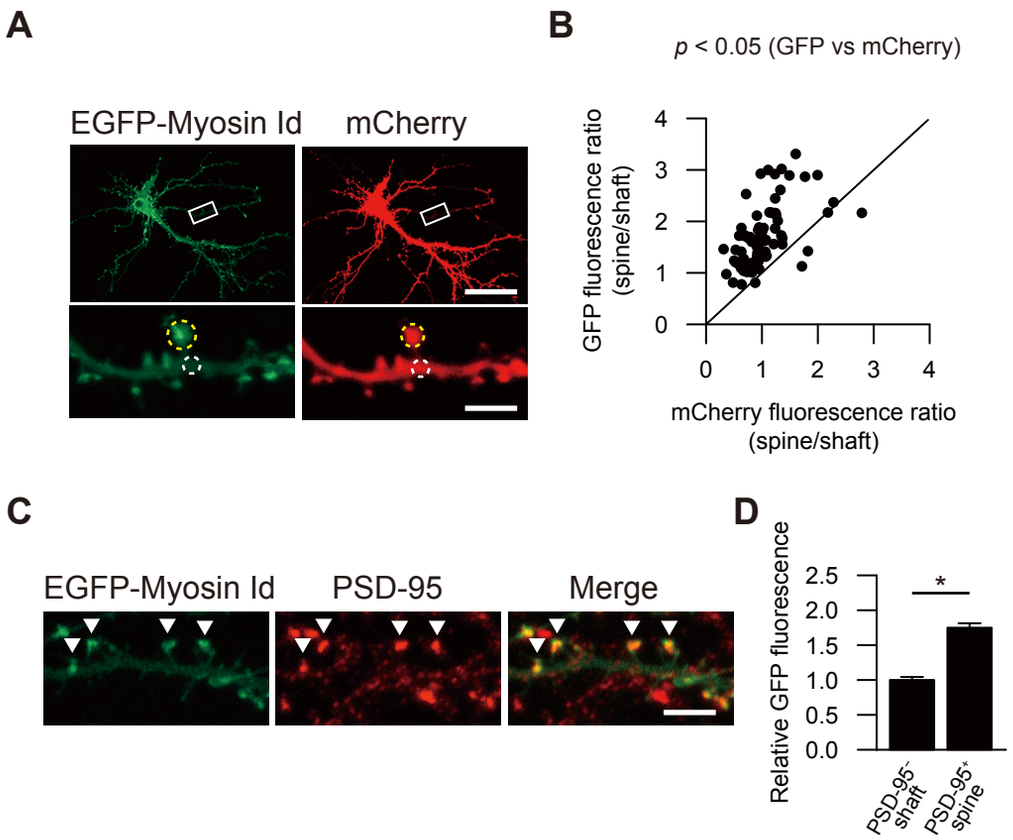

Koshida et al., Fig 4.

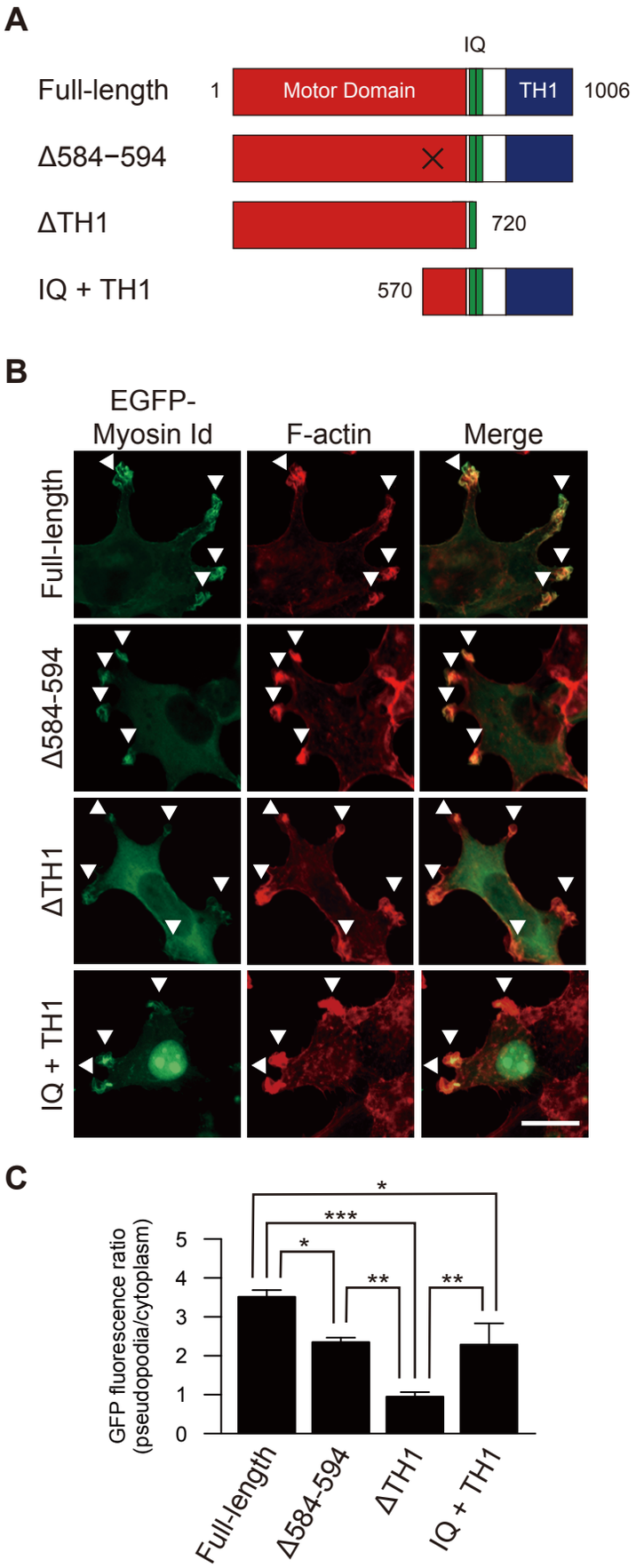

Koshida et al., Fig 5.

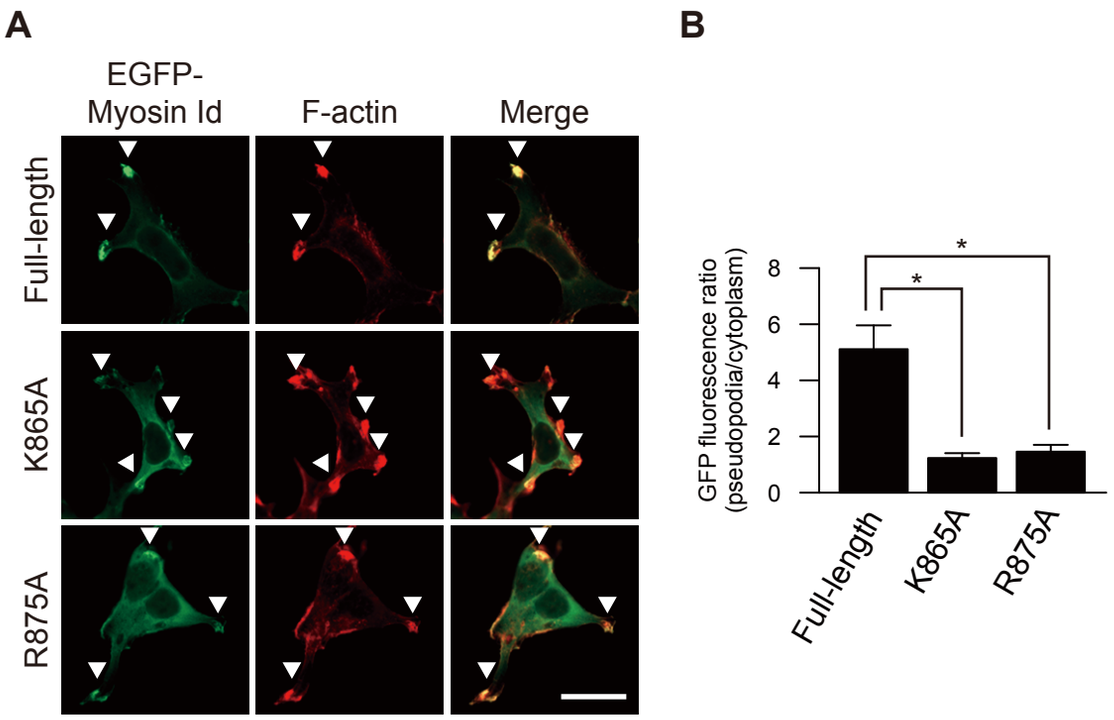

Koshida et al., Fig 6.